

A Comparative Study of the Confinement Models of High-Strength Steel Fiber Concrete by Statistical Approach

Nur Fithriani F. Cholida^{1,*}, Antonius², Lintang Enggartiasto¹

¹Department of Civil Engineering, Universitas Semarang, Semarang, INDONESIA
Jl. Soekarno-Hatta, Universitas Semarang

²Department of Civil Engineering, Universitas Islam Sultan Agung, Semarang, INDONESIA
Jl. Raya Kaligawe Km.04, Semarang

*Corresponding author: tiafithria@gmail.com

SUBMITTED 17 February 2022 REVISED 29 May 2022 ACCEPTED 10 June 2022

ABSTRACT Since the last four decades, the behavior of concrete contains of steel fiber, or often called steel fiber concrete, with a wide range of compressive strength has been carried out. Generally, the results of the experimental program produced a material which has a more ductile compared with normal concrete or concrete without fiber. Due to the ductility properties of the material, it is very suitable for use as an earthquake-resistant structural material. At the same time, the behavior of high-strength steel-fiber concrete has also investigated, one of which is about confined high-strength steel-fiber concrete. Analytical models of confined high-strength steel fiber concrete have been developed in various preliminary studies, with their characteristics derived based on the experimental results. Therefore, this research evaluated the models of confined high-strength steel-fiber concrete proposed by Mansur *et al.*, Hsu and Hsu, and Paultre *et al.* The evaluation includes stress-strain behavior, strength enhancement of confined concrete (f_{cc}/f_{co}) or K value, the increase in confined concrete strain ($\epsilon'_{cc}/\epsilon'_{co}$), and strain of confined concrete when the stress has dropped by 50 percent against its unconfined strain ($\epsilon_{cc50}/\epsilon_{c50}$). The comparison method was carried out using a statistical approach and stress-strain simulation. Evaluation results showed significant predictive differences in confinement models in terms of post-peak behavior and parameters $\epsilon'_{cc}/\epsilon'_{co}$ and $\epsilon_{cc50}/\epsilon_{c50}$. Prediction of confinement models on the value of f_{cc}/f_{co} to the experimental results has a coefficient of variation above 10%. The result further showed that a modified model of confined high-strength steel-fiber concrete was proposed and able to simulate the stress-strain behavior.

KEYWORDS Confinement Models; Steel Fiber; High-strength Concrete; Stress-strain; Coefficient of Variation.

© The Author(s) 2020. This article is distributed under a Creative Commons Attribution-ShareAlike 4.0 International license.

1 INTRODUCTION

It is a generally known fact that high strength concrete (HSC) or those with compressive strength (f_c) of 50 MPa and above has several advantages such as greater crack capacity, relatively low shrinkage, and durable properties (Nishiyama, 2009; Antonius, 2014a; 2014b). However, these substances also have certain weaknesses, namely brittleness, and low ductility. A high-volumetric reinforcement ratio or a more tightly-spaced lateral one is needed to overcome this inconsistency (Paultre and Legeron, 2008; Antonius and Imran, 2012; Cholida *et al.*, 2018). Furthermore, other technological developments, namely concrete-reinforcing fibers, are also required. The addition of certain percentages to the mixture is known to increase the strength, shear capacity, and, more importantly, ductility (Aoude

et al., 2014; Han *et al.*, 2015; Lee *et al.*, 2015; Rosidawani *et al.*, 2017; Hanif and Kanakubo, 2017; Janani and Santhi, 2018; Amariansah and Karlinasari, 2019). Steel fiber concrete, including its behavior at high temperatures, has also been extensively studied and reportedly has good ductility (Korsun *et al.*, 2015; Antonius *et al.*, 2014; 2019).

A combination of HSC and steel fiber is an ideal material for structural components such as the types of columns erected in earthquake zones. One of the advantages is that it reduces the lateral reinforcement ratio, and a good level of ductility is maintained. Various studies reported that this combination exhibits extraordinary stress-strain behavior in strength and ductility (Antonius, 2015; Liu *et al.*, 2018). Several high-strength fiber concrete confinement models have also been de-

signed based on the experimental analyses of diverse studies (Mansur *et al.*, 1997; Hsu and Hsu, 1994; Paultre *et al.*, 2010). Presently, none of them are widely accepted or referred to during planning. Similar lateral or confining reinforcement designs in steel fiber concrete are yet to be regulated based on the existing standard (Indonesian National Standard, 2019).

The confinement model is useful in predicting the behavior of the structure as a whole and providing assurance in terms of the structural design. This research compares the confined high-strength fiber concrete models to evaluate their sensitivity concerning the experimental results used to predict their pre- and post-peak behaviors. The three models selected in this process were designed by Mansur *et al.*, Hsu and Hsu, and Paultre *et al.* The reviewed parameters are stress-strain behavior, strength enhancement of confined concrete

(f'_{cc}/f'_{co}) or K value, the increase in confined concrete strain ($\epsilon'_{cc}/\epsilon'_{co}$), and strain of confined concrete which the stress was dropped by 50 percent against its unconfined strain ($\epsilon_{cc50}/\epsilon_{c50}$).

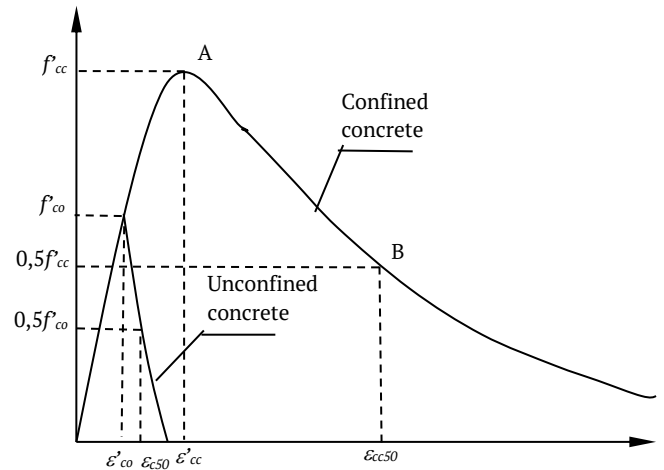


Figure 1. Parameters and curves of the confined concrete

Table 1. Stress-strain models of confined high-strength steel fiber concrete

| Model | Pre and post-peak curves | Stress and strain enhancement | Parameters |
|-----------------------|---|---|---|
| Mansur <i>et al.</i> | $f_c = f'_{cc} \left[\frac{\beta \left(\frac{\epsilon_c}{\epsilon'_{cc}} \right)}{\beta - 1 + \left(\frac{\epsilon_c}{\epsilon'_{cc}} \right)^\beta} \right]$ $f_c = f'_{cc} \left[\frac{k_1 \beta \left(\frac{\epsilon_c}{\epsilon_{cc}} \right)}{k_1 \beta - 1 + \left(\frac{\epsilon_c}{\epsilon_{cc}} \right)^{k_2 \beta}} \right]$ | $\frac{f'_{cc}}{f'_o} = 1 + 0.60 \left(\rho_s \frac{f_y}{f'_o} \right)^{1.23}$ $\frac{\epsilon_{cc}}{\epsilon_o} = 1 + 2.6 \left(\rho_s \frac{f_y}{f'_o} \right)^{0.8}$ | $\beta = \frac{1}{1 - \frac{f'_{cc}}{\epsilon_{cc} \cdot E_{ti}}}$ $k_1 = 2.77 \left(\rho_s \frac{f_y}{f'_o} \right)$ $k_2 = 2.19 \left(\rho_s \frac{f_y}{f'_o} \right) + 0.17$ |
| Hsu and Hsu | $\eta = \frac{nx}{n\beta - 1 + x^{n\beta}}$ $0 \leq x \leq x_d$ | $f'_{cc} = 197.95\rho + f'_c \text{ (in ksi)}$ $\epsilon'_{cc} = 0.2252\rho + \epsilon_o$ <p>The equations above are for the steel fiber content of 0.5%</p> | $\eta = \frac{f_c}{f'_c} ; x = \frac{\epsilon}{\epsilon_o}$ $\beta = \frac{1}{1 - \frac{f'_c}{\epsilon_o E_{ti}}}$ |
| Paultre <i>et al.</i> | $f_c = f'_{cc} \left[\frac{k \left(\frac{\epsilon_c}{\epsilon'_{cc}} \right)}{k - 1 + \left(\frac{\epsilon_c}{\epsilon'_{cc}} \right)^k} \right]$ $f_c = f'_{cc} \exp \left[k_1 (\epsilon_c - \epsilon'_{cc})^{k_2} \right]$ | $\frac{f'_{cc}}{f'_c} = 1 + 2.4 (I'_e)^{0.7}$ $\epsilon'_{cc} = \epsilon'_c + 0.21 (I'_e)^{1.7}$ $I'_e = \frac{f'_{le}}{f'_c}$ | $k = \frac{E_c}{E_c - \left(\frac{f'_{cc}}{\epsilon'_{cc}} \right)}$ $k_1 = \frac{\ln 0.5}{(\epsilon_{cc50} - \epsilon'_{cc})^{k_2}}$ $k_2 = 0.58 + 60 (I_{e50})^{1.4}$ |

2 MODELS OF CONFINED HIGH-STRENGTH STEEL FIBER CONCRETE

Figure 1 shows some parameters that affect the stress-strain behavior of confined concrete. This includes the peak stress of confined concrete (f'_{cc}), peak strain of confined concrete corresponding to the f'_{cc} (ϵ'_{cc}), and strain after stress drop of 50% at descending curve (ϵ'_{cc50}).

The confinement models reviewed in this research have several parameters that tend to affect the stress-strain of confined steel fiber concrete shown in Table 1. In general, all three produced similar non-linear stress-strain curves, as shown in Figure 1.

2.1 Model by Mansur *et al.*

Mansur *et al.* proposed the stress-strain equation concerning confined fiber concrete by testing specimens with strengths between 60 to 120 MPa. The variables reviewed in this analysis include the diameter of the lateral reinforcement, spacing, the concrete core's area, and the specimen casting's direction. It was concluded that the vertical-cast concrete undergoes a considerable strain at maximum stress, while a more remarkable increase in ductility tends to occur in the horizontal-cast concrete. The magnitude of the peak stress and strain and the ductility of the confined concrete is influenced by a specific factor called the confinement parameter. It describes the amount of confinement exerted on the concrete core and is expressed as follows:

$$\text{Confinement parameter} = \rho_s \frac{f_y}{f_o} \quad (1)$$

The strength enhancement of confined concrete (K):

$$K = \frac{f'_{cc}}{f_o} = 1 + 0.60 \left(\rho_s \frac{f_y}{f_o} \right)^{1.23} \quad (2)$$

The peak strain of confined concrete (ϵ_{cc}) in table 1 applies to the vertical-cast concrete. However, for the horizontal-cast concrete, the value of cc is calculated using the following Equation:

$$\frac{\epsilon_{cc}}{\epsilon_o} = 1 + 5.9 \left(\rho_s \frac{f_y}{f_o} \right)^{1.5} \quad (3)$$

The parameters f_o and ϵ_o in the previous equation are the peak stress and strain on the unconfined concrete. The stress-strain equation of confined concrete is shown in Table 1. The β factor is the amount that determines the curve of the slope before the peak response. The stress-strain equation is influenced by the correction factors k_1 and k_2 .

According to Mansur *et al.*, changes in the diameter of the lateral reinforcement, spacing, and the concrete core area greatly affect the shape of the downward curve after the peak. The variables that considerably affect the ductility of the confined concrete are properly represented by the confinement parameter, namely the $\rho_s f_y / f_o$ factor.

1.2 Model by Hsu and Hsu

Hsu and Hsu proposed an empirical stress-strain equation for high-strength steel fiber concrete, where the compressive strength of the design is approximately 10,000 psi (68 MPa). This was derived from the test results obtained from a cylinder consisting of unconfined and confined high-strength steel fiber concrete, with an inner diameter and height of 3 inches and 6 inches, respectively. Steel fiber concrete is designed with varying fiber fraction (V_f) volumes of 0, 0.5, 0.75, and 1%. The confined type uses hoop reinforcement with space variations of 1, 2, and 3 inches.

Based on Table 1, Hsu and Hsu applied an unconfined and confined concrete stress-strain equation, an empirical modification proposed by Carreira and Chu (1985) and Ezeldin and Balaguru (1992). Hsu and Hsu explained that n and β are material parameters in which β controls the shape of the stress-strain curve, n and x are the normalized stress and strain, respectively. Factor of β also influences the value of the initial tangential modulus (E_{it}) and concrete compressive strength (f'_c). Furthermore, f'_c and ϵ_c are general stresses and strains, respectively. f'_c is the peak stress and ϵ_o is the strain when the concrete reaches the peak stress. x_d is the strain when the stress has dropped to 60% of its peak (on the descending curve). The proposed model by Hsu and Hsu assumed that the peak stress and

strain of the confined concrete depended on the lateral reinforcement ratio and the compressive strength of the unconfined type.

1.3 Model by Paultre *et al.*

Paultre *et al.* developed a confinement model for high-strength steel-fiber concrete ($80 \leq f'_c \leq 100$ MPa), and it was based on the test results of the full-scale column. The parameters reviewed in the experiment include concrete compressive strength, volumetric ratio, spacing and yield stress of lateral reinforcement, configuration, and steel fiber volume fraction. The column specimens studied comprised 15 pieces, and all of them used a concrete blanket of cross-sectional size 235x235 mm, and a total height of 1400 mm, where the test region was set at 900 mm. The volume variation of the steel fiber fraction is 0.25, 0.5, 0.75, and 1%, where the length to diameter (l/d) ratio is 50. The volumetric ratio of lateral reinforcement varies from 2.5 to 3.4%.

The stress-strain curve proposed by Paultre *et al.* consists of pre-and post-peak equations. Based on Table 1, the strength enhancement of confined concrete ($K=f'_{cc}/f'_{co}$) is a function of the confinement index (I_e) and effective lateral stress (f'_{le}). In addition, the longitudinal reinforcement ratio varies from 2.2 to 3.6%, and the yield stresses of the ties used are 400 and 800 MPa. From Table 1, it can be identified that the peak stress and strain of confined concrete represent a function of the effective confinement index (I_e'). Meanwhile, the effective lateral stress (f'_{le}) is obtained using Equation 4:

$$f'_{le} = K_e \frac{A_{sh}}{sc} f_h = \rho_{sey} f_h \quad (4)$$

where c is the concrete core size (center to center of the ties), A_{sh} is the total cross-section area of the ties in the y -direction, f_h is the lateral steel stress at the concrete peak stress, and ρ_{sey} is the effective sectional ratio of the confining reinforcement. $\rho_{sey} = K_e A_{sh} / (sc)$ in the y -direction, where K_e is the effective confined area, according to Mander *et al.* (1988).

Paultre *et al.* proposed to compute the stress of lateral reinforcement at peak response (f'_h) as shown in Equations 5 and 6:

$$f'_h = f_{yh} ; \text{ if } \kappa \leq 10 \quad (5)$$

$$f'_h = \frac{0.25 f'_c + 10 \eta_\theta \tau_{fu} V_f (l_f / d_f)}{\rho_{sey} (\kappa - 10)} \geq 0.43 \varepsilon'_c E_s \leq f_{yh} \quad (6)$$

if $\kappa > 10$

τ_{fu} is a constant frictional bond strength, and η_θ is defined as the fiber orientation efficiency factor. Paultre *et al.* stated that the κ factor is used to determine whether or not the ties' reinforcement yielded at the peak stress, where:

$$\kappa = \frac{f'_c}{\rho_{sey} E_s \varepsilon'_c} \quad (7)$$

However, assuming the cross-section is circular or square, then the effective ratio (ρ_{sey}) of the reinforcement bars is:

$$\rho_{sey} = \frac{I}{2} K_e \rho_s \quad (8)$$

Table 1 shows that I_{e50} is the lateral stress due to the installed reinforcement with fiber and is calculated as follows:

$$I_{e50} = \frac{\rho_{sey} f_{hy}}{f'_c} + \frac{\eta_{50} \eta_\theta \tau_{fu} V_f (l_f d_f)}{f'_c} \quad (9)$$

Paultre *et al.* proposed Equation (9), where η_{50} is the parameter that considers the fibers' influence when the axial strain is equal to that of the post-peak (ε_{cc50}). Moreover, the concrete strain when the peak stress drops by 50% during post-peak is calculated as follows:

$$\varepsilon_{cc50} = \varepsilon_{c50} + 0.15 (I_{e50})^{1.1} \quad (10)$$

Where ε_{c50} is defined as post-peak strain corresponding to the stress, which is equal to 50% of the unconfined concrete strength.

3 COMPARISON BETWEEN CONFINEMENT MODELS WITH EXPERIMENTS

The confinement models earlier presented were evaluated concerning the confined steel fiber concrete. The experimental data used are the results of Antonius' experimental study (2015), carried out on the behavior of normal and high-strength steel fiber concrete with circular sections confined by hoops (Figure 2). There were 12 small-scale specimens with a diameter of 125 mm and a height of 310 mm. Strength behavior and energy absorption ability of confined steel fiber concrete are the main focus of this research. Specimens were grouped into two primary categories to evaluate the presence of fiber. This includes those without fiber ($V_f = 0\%$) and those with fiber of (V_f) 0.5% following the concrete volume. Its compressive strength varies from 29 to 72 MPa, and the hoop reinforcement characteristics have a spacing (s) of 60 to 100 mm. All hoop reinforcement has similar yield stress (f_y) of 430 MPa, while that of the longitudinal is 6D5.5. All test specimens were made without a concrete cover. Antonius further stated that the stress-strain behavior of high-strength steel fiber reinforced concrete is significantly different, especially its post-peak behavior. Therefore, the existing confinement model was modified to obtain a more reliable prediction.

Antonius' experimental data are shown in Table 2. In this study, the modified confined steel fiber concrete is compared to Antonius' experimental results, particularly for the specimens ($V_f=0.5\%$). Therefore, those used as validation are FC3, FC4, FC5, FC6, FC7, FC8, and FC9. The peak stress value of unconfined concrete is $0.85f_c$. The peak strain (ϵ_{co}) for normal, medium, and high strength concrete are 0.0037, 0.0035, and 0.0032, respectively. The parameters ϵ_{cc50} and ϵ_{c50} refer to the data obtained from the research conducted by Antonius *et al.* (2014).

The lateral stress proposed by Paultre *et al.*, as shown in Equation (9), applies to specimens with square sections. For circular sections, the modified lateral stress is as follows:

$$f_l = \frac{2A_{sh}f_y}{sd_c} + \frac{\eta_{50}\eta_{\theta}\tau_{fu}v_f(l_f d_f)}{f_c} \tag{11}$$

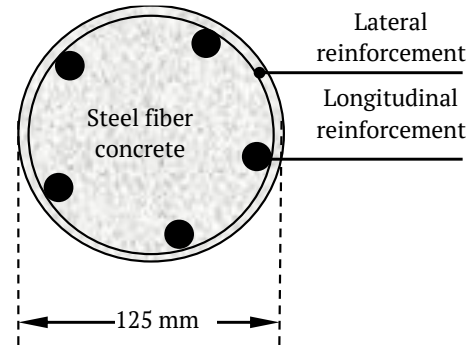


Figure 2. Cross-section of specimen

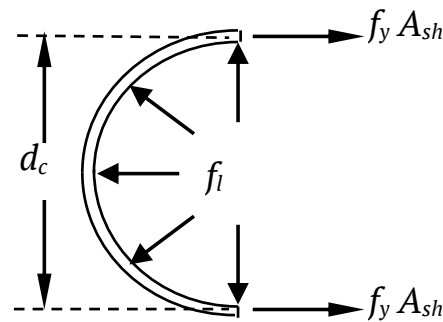


Figure 3. Equilibrium forces of confinement

Meanwhile, $2A_{sh}f_y/sd_c$ is based on the equilibrium of the forces acting on the half-turn of hoops in Figure 3. In Equation (11), the lateral stresses are corrected by the effectiveness of confinement based on the concept designed by Mander *et al.* (1988). A comparison of the confinement models with experimental (exp.) results was carried out using a statistical approach. The differences were stated in accordance with the coefficient of variation (COV) and stress-strain behavior of confined concrete.

Table 2. Experimental result by Antonius (2015)

| Specimen | f'_c (MPa) | V_f (%) | Confining reinforcement | | | Long. Reinf. | f'_{cc} (MPa) | ϵ'_{cc} | K |
|----------|-----------------|--------------|-------------------------|-----------------------|----------------|-----------------|--------------------|------------------|------|
| | | | ϕ -s (mm) | Ratio (ρ_h) | f_y (MPa) | | | | |
| UFC30 | 29.5 | | - | - | - | | - | - | - |
| UFC50 | 51 | 0.5 | - | - | - | | - | - | - |
| UFC70 | 71.2 | | - | - | - | | - | - | - |
| FC1 | 51 | 0 | 6-60 | 1.58 | | 6D5.5 | 57 | 0.0044 | 1.56 |
| FC2 | 71.2 | 0 | 6-60 | 1.58 | | | 79.27 | 0.0055 | 1.31 |
| FC3 | 29.5 | | 6-60 | 1.58 | | $f_y=$ | 35.25 | 0.0110 | 1.36 |
| FC4 | 29.5 | | 6-100 | 0.95 | 415 | 430 | 30.22 | 0.0058 | 1.17 |
| FC5 | 51 | 0.5 | 6-60 | 1.58 | | MPa | 53,5 | 0.0075 | 1.24 |
| FC6 | 51 | | 6-100 | 0.95 | | | 48.52 | 0.0051 | 1.12 |
| FC7 | 51 | | 5.5-60 | 1.33 | | | 55.53 | 0.0076 | 1.28 |

4 RESULTS AND DISCUSSION

Table 3. Statistical results for f'_{cc}/f'_{co} , $\epsilon'_{cc}/\epsilon'_{co}$, $\epsilon_{cc50}/\epsilon_{c50}$

| Specimen | f'_{cc}/f'_{co} | | | | $\epsilon'_{cc}/\epsilon'_{co}$ | | | | $\epsilon_{cc50}/\epsilon_{c50}$ | | | |
|----------|-------------------|--------|-------|---------|---------------------------------|--------|-------|---------|----------------------------------|--------|--------|---------|
| | Exp. | Mansur | Hsu | Paultre | Exp. | Mansur | Hsu | Paultre | Exp. | Mansur | Hsu | Paultre |
| FC3 | 1.36 | 1.12 | 1.86 | 1.56 | 2.2 | 0.335 | 0.64 | 0.726 | 7 | - | 14.319 | 0.658 |
| FC4 | 1.17 | 1.06 | 1.52 | 1.37 | 1.16 | 0.213 | 0.058 | 0.035 | 3.8 | - | 0.341 | 5.707 |
| FC5 | 1.24 | 1.06 | 1.34 | 1.38 | 1.875 | 0.05 | 0.226 | 0.278 | 7.375 | - | 17.297 | 0.084 |
| FC6 | 1.12 | 1.03 | 1.14 | 1.25 | 1.275 | 0.361 | 0.144 | 0.005 | 3.475 | - | 0.067 | 11.621 |
| FC7 | 1.28 | 1.05 | 1.26 | 1.35 | 1.9 | 0.010 | 0.014 | 0.305 | 4.875 | - | 2.752 | 5.240 |
| FC8 | 1.25 | 1.04 | 1.21 | 1.30 | 2.5 | 0.144 | 0.36 | 1.327 | 7.975 | - | 22.648 | 0.036 |
| FC9 | 1.15 | 1.03 | 1.15 | 1.28 | 1.425 | 0.231 | 0.068 | 0.006 | 5 | - | 3.183 | 4.792 |
| Mean | | 1.06 | 1.35 | 1.357 | | 1.621 | 1.4 | 1.348 | | - | 3.216 | 6.189 |
| SD | | 0.201 | 0.165 | 0.166 | | 0.467 | 0.502 | 0.669 | | - | 3.178 | 2.166 |
| COV (%) | | 19.05 | 12.18 | 12.23 | | 28.80 | 35.83 | 49.60 | | - | 98.83 | 34.99 |

4.1 Statistical Analysis

Table 3 shows the statistical analysis results performed on confinement models and the varying experiments. The value of K or strength enhancement of confined concrete (f'_{cc}/f'_{co}) is an important parameter because it is used to determine the minimum volumetric reinforcement ratio in the design. The prediction of K values based on the models designed by Mansur *et al.*, Hsu and Hsu, and Paultre *et al.* and their experimental results has COVs of 19.05%, 12.18%, and 12.23%. As shown in Table 3, the average error of Mansur's model prediction is the highest compared to the

others. The prediction of the K value of each model is relatively distinct from each experimental result. On the contrary, $\epsilon'_{cc}/\epsilon'_{co}$ based on the Mansur *et al.* model is the closest to the experimental results (COV = 28.80%). Table 3 shows that the COV value based on the Hsu and Hsu and Paultre *et al.* models is 35.83% and 49.60%, respectively.

Furthermore, the forecast value and that of $\epsilon_{cc50}/\epsilon_{c50}$ were compared. The predictions of the Mansur *et al.* model were not calculated because the value of ϵ_{cc50} was unable to be determined. Figures 4 to 6 show that the curves after the peak

stress process failed to decrease by less than 10% significantly. On the contrary, the predicted value of $\epsilon_{cc50}/\epsilon_{c50}$ based on the Hsu and Hsu model has a significant COV value of 98.83%, following Paultre *et al.*, which is below 34.99%. These indicate a significant difference between the predictions of confinement models and the results of experiments on the descending branch curve.

4.2 Stress-strain Behavior

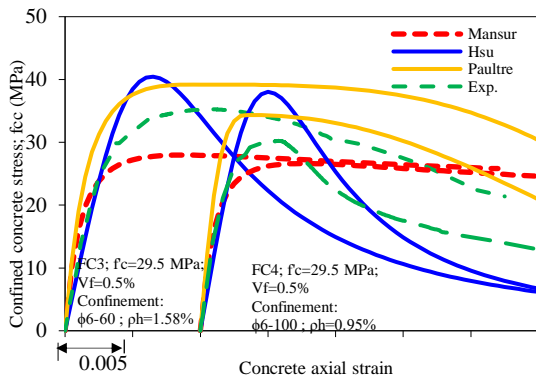


Figure 4. Comparison of confined concrete models with specimen of FC3 and FC4

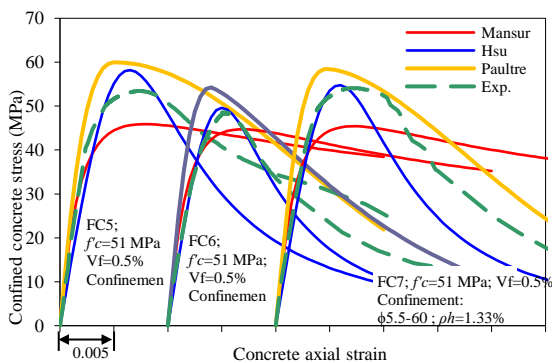


Figure 5. Comparison of confined concrete models with specimen of FC5, FC6, and FC7

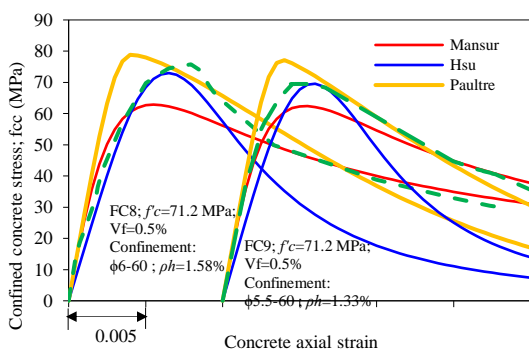


Figure 6. Comparison of confined concrete models with specimen of FC8 and FC9

Figures 4 to 6 show the confined stress-strain curves of the three models and the experimental results for all specimens. Besides from that of Paultre *et al.*, it was generally reported that the ascending branch curve of the two other models is quite close to that of the experimental data. Paultre *et al.* research have higher initial stiffness and a steeper ascending curve than the other models. Another observed phenomenon is the existence of a significant difference between all descending branch curves and that of the experiments. This is in line with the results of the statistical analysis earlier obtained, where the value of COV in the $\epsilon_{cc50}/\epsilon_{c50}$ of either model by Hsu and Hsu or Paultre *et al.* is extremely large (98.83% and 34.99%). The COV value based on the Mansur *et al.* model was unpredictable due to the large difference between $\epsilon_{cc50}/\epsilon_{c50}$ and the experiment.

As earlier explained, the prediction of the f'_{cc} value according to the model designed by Mansur *et al.* is entirely different from the experimental results. It could only be used to accurately forecast the f'_{cc} values of FC4 and FC7 specimens, as shown in Figures 4 and 5. However, in another figure, the value of f'_{cc} in the Mansur *et al.* model and the experiment is different.

| | | | |
|---------|------|-------|-------|
| COV (%) | 8.30 | 32.07 | 34.14 |
|---------|------|-------|-------|

In a normal-strength steel fiber concrete ($f'_c = 29.5$ MPa), the model proposed by Hsu and Hsu is used to predict inaccurate experimental f'_{cc} values (Figure 4). Its accuracy in predicting the value of the new f'_{cc} is evident in high-strength steel fiber concrete, as shown in Figures 5 and 6. Although, the model by Paultre *et al.* was used to overestimate the f'_{cc} value for all specimens. In predicting the value of ϵ'_{cc} based on all the confinement models, none of them coincides with the experimental ϵ'_{cc} , and the difference is quite much (COV greater than 28%).

5 PROPOSED MODIFIED MODEL

The comparisons among the confinement models significantly reflect the differences between the confined concrete specimens and the experimental results. It is necessary to modify that of the steel fiber, thereby ensuring that the differ-

ence is relatively close. Based on all the confinement models, it is evident that the descending branch of those designed by Hsu and Hsu and Paultre *et al.* has a shape that is almost similar to that of the experiment, especially for confined high-strength steel fiber concrete. However, the descending branch of the model designed by Hsu and Hsu tends to be sharper or steeper than that of Paultre *et al.*, which is also indicated by the large value of COV of the $\epsilon_{cc50}/\epsilon_{c50}$ parameter. Based on this, the Paultre *et al.* model was adopted by modifying several parameters.

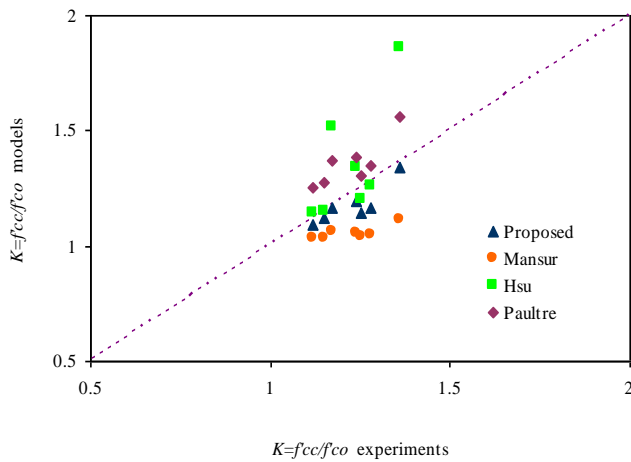


Figure 7. *K* value between models with experiments

Table 4. COV value is based on the proposed model of the experiment

| Specimen | Proposed | | | |
|----------|----------|-------------------|---------------------------------|----------------------------------|
| | Exp. | f'_{cc}/f'_{co} | $\epsilon'_{cc}/\epsilon'_{co}$ | $\epsilon_{cc50}/\epsilon_{c50}$ |
| FC3 | 1.36 | 1.34 | 0.296 | 0.872 |
| FC4 | 1.17 | 1.16 | 0.037 | 6.947 |
| FC5 | 1.24 | 1.20 | 0.427 | 1.030 |
| FC6 | 1.12 | 1.09 | 0.007 | 8.649 |
| FC7 | 1.28 | 1.17 | 0.322 | 5.061 |
| FC8 | 1.25 | 1.14 | 0.660 | 0.588 |
| FC9 | 1.15 | 1.12 | 0.063 | 3.897 |
| Mean | | 1.175 | 1.713 | 6.218 |
| SD | | 0.098 | 0.550 | 2.13 |

The first modification was to change the equation of the *K* value. A linear equation was proposed based on the triaxial testing of steel fiber concrete by Pantazopoulou and Zanganeh (2001), as stated in Equation (12).

$$K = \frac{f'_{cc}}{f'_{co}} = 1 + 3.5 \frac{f_l}{f'_{co}} \tag{12}$$

The second modification is centered on the lateral stress calculations in Equation (11), where the effect of fiber was included. Therefore, the lateral stress calculation is :

$$f_l = \frac{2A_{sh}f_y}{sd_c} \tag{13}$$

Additionally, the equation of the *K* value based on the proposed model and other confinement types was compared with the experiments of all specimens. Figure 7 shows that the proposed formula for *K* values is relatively close to the diagonal, indicating that it is quite good.

Statistical analysis between the proposed model and the complete experiment is shown in Table 4. The COV value of the predicted *K* value is relatively 8.30%, while that of the following parameters, namely, $\epsilon'_{cc}/\epsilon'_{co}$ and $\epsilon_{cc50}/\epsilon_{c50}$ are 32.07% and 34.14%, respectively. Validation of confined steel fiber concrete stress-strain curves is shown in Figures 8 to 10. In normal strength concrete validation (Figure 8), the behavior of the curve after the peak of the proposed model is relatively close to that of the experiment, even though its shape is not identical. This is because the proposed model is for confined-high strength steel fiber concrete.

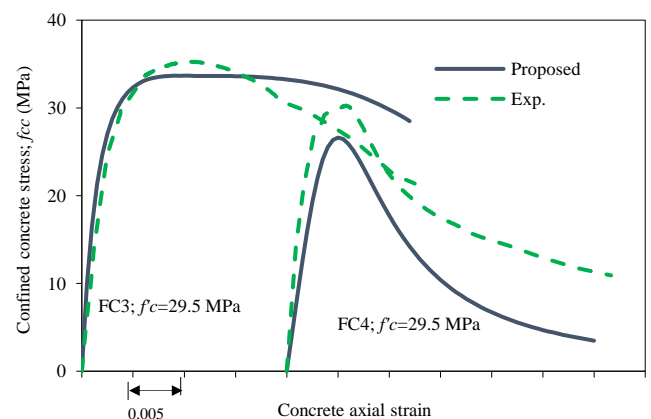


Figure 8. Proposed model vs Exp. (FC3 and FC4)

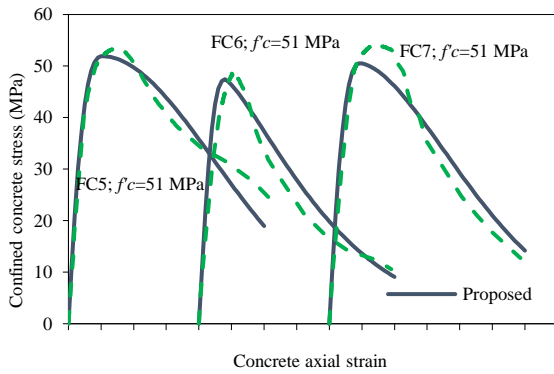


Figure 9. Proposed model vs Exp. (FC5, FC6 and FC7)

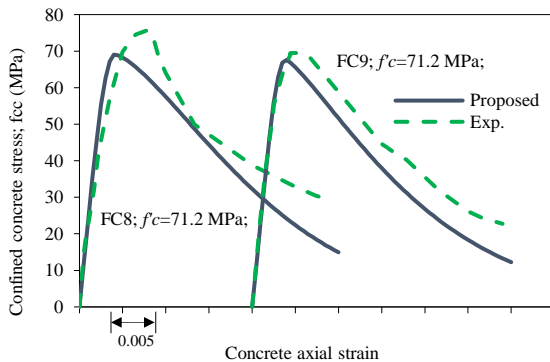


Figure 10. Proposed model vs Exp. (FC8 and FC9)

A comparison of steel fiber concrete stress-strain curves with 51 MPa compressive strength shows that the pre-and post-peak curves between the proposed models and experiments are extremely close (Figure 9). This is similar to the comparison with higher concrete strength ($f'_c=71.2$ MPa), as shown in Figure 10. These indicate that the proposed model can accurately predict the stress-strain behavior of confined high-strength steel fiber concrete.

6 CONCLUSION

The predicted and experimental values of confined fiber concrete (K) strength enhancement ranged between 12 to 20 percent. These indicate that there is an inaccurate estimate of the K value. Correlations of the $\epsilon'_{cc}/\epsilon'_{co}$ and $\epsilon_{cc50}/\epsilon_{c50}$ between confinement models and the experiments did not align. Therefore, the confinement models predicting the strains after peak response are inaccurate. Their ascending branch behaviors are also relatively similar, except for the prediction of the model designed by Paultre *et al.*, which tends to be different. The descending branches between confinement models and the

experiment are rather different. However, even though the shape of the descending branch curve by Hsu and Hsu and Paultre *et al.* is comparable to the experiment. Paultre *et al.* confinement model was adopted and used to develop a confined steel fiber concrete proposition specimen. Its modification is based on the equation used to calculate K proposed by Pantazopoulou and Zanganeh. Lateral stress only pays attention to the confinement action by the reinforcement. The proposed model can accurately predict the experiment's K value (COV=8.30%). It can also properly simulate the ascending and descending branches of the experiment, especially for confined high-strength steel fiber concrete.

DISCLAIMER

The authors declare no conflict of interest.

ACKNOWLEDGMENT

The authors are grateful to the Directorate of Higher Education Republic of Indonesia for funding this research through the Competitive Research Program, Contract No.002/K6/KL/SP/PEN/2014, used to validate the confinement models.

REFERENCES

- Amariansah, W. and Karlinasari, R. (2019). The Influence of Steel Fiber on the Stress-Strain Behavior of Confined Concrete. *Journal of Advanced Civil and Environmental Engineering*, 2, pp. 46-52.
- Antonius, Widhianto, A., Darmayadi, D. and Asfari, G.D. (2014). Fire Resistance of Normal and High-Strength Concrete with Contains of Steel Fibre. *Asian Journal of Civil Engineering*, 15, pp. 655-669.
- Antonius, and Imran, I. (2012). Experimental Study of Confined Low-, Medium- and High-Strength Concrete Subjected to Concentric Compression. *ITB Journal of Engineering Science*, 44, pp. 252-269.
- Antonius, Purwanto and Harprastanti, P. (2019). Experimental Study of the Flexural Strength and Ductility of Post Burned Steel Fiber RC Beams. *International Journal of Technology*, 10, pp. 428-437.

- Antonius (2015). Strength and Energy Absorption of High-Strength Steel Fiber Concrete Confined by Circular Hoops. *International Journal of Technology*, 6, pp. 217-226.
- Antonius (2014a). Performance of High-Strength Concrete Columns Confined by Medium Strength of Spirals and Hoops. *Asian Journal of Civil Engineering*, 15, pp. 245-258.
- Antonius (2014b). Studies on the Provisions of Confining Reinforcement for High-Strength Concrete Column. *Procedia Engineering*, 95, pp. 100-111.
- Antonius, Imran, I. and Setiyawan, P. (2017). On the Confined High-Strength Concrete and Need of Future Research. *Procedia Engineering*, 171, pp. 121-130.
- Aoude, H., Hosinie, M.M., Cook, W.D. and Mitchell, D. (2014). Behaviour of Rectangular Columns Constructed with SCC and Steel Fibers. *Journal of Structural Eng.*, September.
- Antonius, Karlinasari, R. and Darmayadi, D. (2014). Confinement Model for Steel Fiber Concrete. Report of Competitive Research, Directorate General of Higher Education (in Indonesian).
- Carreira, D. J., and Chu, K.-H. (1985). Stress-Strain Relationship for Plain Concrete in Compression. *ACI Journal*, 82, pp. 797-804.
- Cholida, N.F.F., Antonius and Ni'am, F. (2018). A Parametric Study of Confinement Effects to the Interaction Diagram of P-M for High-Strength Concrete Columns. *Journal of Advanced Civil and Environmental Engineering*, 1, pp. 30-37.
- Ezeldin, A. S., and Balaguru, P. N. (1992). Normal and High-Strength Fiber Reinforced Concrete under Compression, *Journal of Materials in Civil Engineering*, 4, pp. 415-429.
- Han, A.L, Antonius and Okiyarta, A.W. (2015). Experimental Study of Steel Fiber Reinforced Concrete Beams with Confinement. *Procedia Engineering*, 125, pp. 1030-1035.
- Hanif, F., and Kanakubo, T. (2017). Shear Performance of Fiber-Reinforced Cementitious Composites Beam-Column Joint Using Various Fibers. *Journal of The Civil Engineering Forum*, 3, pp. 113-124.
- Hsu, L.S. and Hsu, C.T. (1994). Stress-Strain Behavior of Steel-Fiber High-Strength Concrete under Compression. *ACI Structural Journal*, 91, pp. 448-457.
- Indonesian National Standard, SNI-2847-2019. Requirements of Structural Concrete for Building and Commentary [in Indonesian].
- Janani, S. and Santhi, A.S. (2018). Multiple Linear Regression Model for Mechanical Properties and Impact Resistance of Concrete with Fly Ash and Hooked-End Steel Fibers. *International Journal of Technology*, 9, pp. 526-536.
- Korsun, V., Vatin, N., Franchi, A., Korsun, A., Crespi, P. and Mashtaler, S. (2015). The Strength and Strain of High-Strength Concrete Elements with Confinement and Steel Fiber Reinforcement Including the Conditions of the Effect of Elevated Temperatures. *Procedia Engineering*, 117, pp. 970-979.
- Liu, Y., Zhu, P. and Wang, W. (2018). Study on Axial Compression Test of Fiber Reinforced High Strength Concrete Column. *AIP Conference Proceedings*, 2036, 030007.
- Lee, S.C., Oh, Joung-Hwan and Cho, Jae-Yeol. (2015). Compressive Behavior of Fiber-Reinforced Concrete with End-Hooked Steel Fibers. *Materials*, 8 pp. 1442-1458.
- Mansur, M.A., Chin, M.S. and Wee, T.H. (1997). Stress-Strain Relationship of Confined High-Strength Plain and Fiber Concrete. *Journal of Materials in Civil Engineering*, 9, pp. 171-179.
- Mander, J.B., Priestley, M.J.N. and Park, R. (1988). Theoretical Stress-Strain Model for Confined Concrete. *Journal of Structural Engineering*, 114, pp. 1804-1824.
- Nishiyama, M. (2009). Mechanical Properties of Concrete and Reinforcement-State-of-the-Art

Report on HSC and HSS in Japan. *Journal of Advanced Concrete Technology*, 7, pp. 157-182.

Pantazopoulou, S.J. and Zanganeh, M. (2001). Tri-axial Tests of Fiber-Reinforced Concrete. *Journal of Materials in Civil Engineering*, 13, pp. 340-348.

Paultre, P. and Legeron, F. (2008). Confinement Reinforcement Design for Reinforced Concrete Columns. *Journal of Structural Eng. ASCE*, 134, pp.738-749.

Paultre, P., Eid, R., Langlois, Y. and Lévesque, Y. (2010). Behavior of Steel Fiber-Reinforced High-Strength Concrete Columns under Uniaxial Compression. *Journal of Structural Engineering*, 136, pp. 1225–1235.

Rosidawani, Imran, I., Pane, I. and Sugiri, S. (2017). Stress-Strain Relationship of Synthetic Fiber Reinforced Concrete Columns. *MATEC Web of Conferences*, 103(02004).

[This page is intentionally left blank]